Available online at www.sciencedirect.com
SCIENCE DIRECT®
Cement and Concrete Research 36 (2006) 1268 – 1278
Cement and Concrete Research

Evaluation of a basic creep model with respect to autogenous shrinkage

Yun Lee [a], Seong-Tae Yi [b], Min-Su Kim [a], Jin-Keun Kim [a,*]

[a] Department of Civil and Environmental Engineering, Korea Advanced Institute of Science and Technology (KAIST), 373-1, Kuseong-dong, Yusong-gu, Daejeon, 305-701, South Korea
[b] Department of Civil Engineering, Chung Cheong University, 330, Wolgok-ri, Kangnae-myun, Cheongwon-kun, Chungbuk-do, 363-792, South Korea

Received 28 December 2005; accepted 14 February 2006

Abstract

This paper shows the results obtained from an experimental study to evaluate a basic creep model. In this study, four different mixture proportions were placed, and tests on the specimens for autogenous shrinkage and basic creep were conducted with respect to age and stress level. The primary test variable was the water/cement ratio (w/c).

From this research, it was found that for low w/c concrete, as well as at an early age of normal-strength concrete, a significant difference exists between apparent basic creep (including autogenous shrinkage) and real basic creep (excluding autogenous shrinkage). Furthermore, creep strain was not directly proportional to the applied stress level after one day. It was also discovered that when the current basic creep model that includes autogenous shrinkage is used in creep analysis, considerable errors as well as some computational problems may result. We therefore recommend modifying the equations of the current basic creep model with respect to autogenous shrinkage.

Keywords: Basic creep; Autogenous shrinkage; Low w/c concrete; Early age

1. Introduction

Autogenous shrinkage of concrete is a phenomenon in which concrete shrinks without any change in mass or temperature. First mentioned by Lyman [1] in 1934, no known research was conducted on this phenomenon for several decades. Since the early 1990s, the importance of autogenous shrinkage has been wholly reconsidered, and now a number of researchers continue to conduct studies on this increasingly important phenomenon [2–6].

Autogenous shrinkage arises from self-desiccation due to water consumption and from the hydration of cementitious materials during the first few hours or days after placement has been completed. Autogenous shrinkage of concrete increases as the water/cement ratio (w/c) decreases [7,8].

Creep in concrete can be divided into two categories: basic creep and drying creep. Westman [9] investigated the early-age creep behavior in compression, and his results showed a strong age dependency on basic creep behavior. In his study, he proposed a method of modeling the early age creep behavior by extending the triple power law. For tensile creep, Østergaad et al. [10] examined the early-age basic tensile creep response through basic creep tests at early ages. Their study showed that a high creep response was produced when the concrete was loaded at early ages, and that the creep response was not directly proportional to the applied stress when the concrete specimen was loaded at one day. Additionally, they formulated a method of describing the early-age tensile creep response by modifying the solidification creep model. Recently, however, Altoubat and Lange [11,12] reported that real basic creep strains could not be measured due to the influence of autogenous shrinkage from sealed specimens. Furthermore, they felt that in order to obtain the real creep strains, compensation for moisture loss due to cement hydration, which was necessary for preventing autogenous shrinkage, should be made.

Fig. 1 shows a schematic relation between real basic creep and autogenous shrinkage. The figure illustrates that real basic creep strains can be obtained by subtracting autogenous shrinkage strains from measured basic creep strains. According to recent studies [13,14], however, the basic creep measured from a sealed concrete specimen is inaccurate. More specifically, for low w/c concrete, the inaccuracy is more apparent due to the autogenous shrinkage that occurs at an early age.

* Corresponding author. Tel.: +82 42 8693614; fax: +82 42 8693610.
E-mail address: kimjinkeun@kaist.ac.kr (J.-K. Kim).

0008-8846/$ - see front matter
doi:10.1016/j.cemconres.2006.02.011

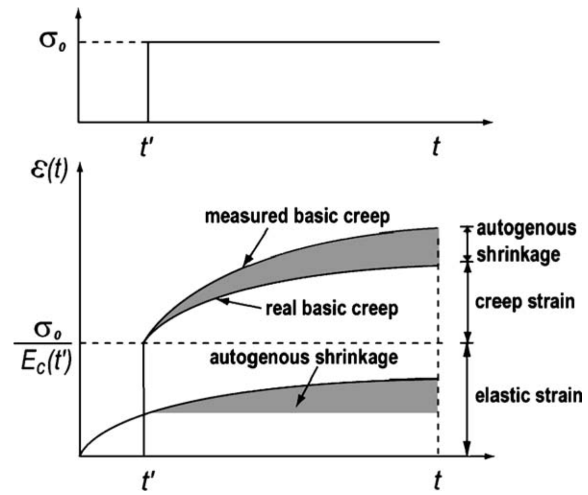

Fig. 1. Time-dependent deformations of the concrete under sustained loads.

The objective of this study was to experimentally and theoretically investigate the necessity of separating autogenous shrinkage from a basic creep model, and to suggest a methodology for this separation. To satisfy this objective, a series of autogenous shrinkage tests and basic creep tests were performed and then the test results were analyzed.

2. Experimental program

2.1. Mixture proportions

Table 1 lists the concrete mixture proportions selected for the autogenous shrinkage and the basic creep test specimens, and the 28-day compressive strength cylinder specimens. In all of the mixtures, ASTM type I Portland cement was used. Crushed gravel was also used as the coarse aggregate, with the maximum aggregate size, d_a, being 19 mm. For good workability and consolidation of the concrete, a super-plasticizer (Super-20), which meets the ASTM C 494 requirements for a Type F admixture [15], was also used. All test cylinders were removed from the mold after 24 h and were wet-cured in a curing room with 100% relative humidity (RH) at 20 °C until the testing date. The compressive strength of concrete was determined in accordance with ASTM C 39 [16].

2.2. Test specimens

For each concrete mixture shown in Table 1, the test specimens used to study the effects of w/c and age; stress level are illustrated in Table 2.

2.3. Test procedures

2.3.1. Autogenous shrinkage tests for various water/cement ratios and ages

Autogenous shrinkage was measured just after casting the 100 mm × 100 mm × 400 mm prism specimen. Fig. 2 is a corresponding schematic diagram.

To eliminate the restraint between the mold and the test specimen, a polytetrafluoroethylene sheet with a low friction coefficient was used. In addition, before the casting, a polyester film was used to prevent the concrete specimen from sticking to the polytetrafluoroethylene sheet. Studs were inserted into the specimen and, before the hardening, the linear variable displacement transducers (LVDTs) installed on each stud were used to measure any deformations.

After hardening, the deformations were measured with embedded strain gages that were positioned at the center of the concrete specimens and oriented along the longitudinal axis of the specimen. Immediately after casting, we began measuring autogenous shrinkage strains of the test specimen. To determine autogenous shrinkage strain, the thermal strain, determined from a thermocouple embedded in the inner part of the concrete specimen, was subtracted from the total strain measured by the embedded strain gage.

2.3.2. Basic creep tests for various water/cement ratios and ages

Basic creep tests were performed on twelve ϕ150 mm × 300 mm cylindrical specimens with stresses applied at 1, 3, 7, and 28 days in a curing room at 20 °C. The test specimens were sealed immediately with a polyester film to prevent the evaporation of moisture from the specimen. After grinding the ends of the specimens, the stress was applied vertically to three identical ϕ150 mm × 300 mm cylinders in which the specimens were aligned in the axial direction with little eccentricity. The applied stress was 30% of the compressive strength of the concrete (i.e., $0.3f'_c$). Again, the thermal strain was subtracted from the total strain.

2.3.3. Autogenous shrinkage tests and basic creep tests for various stress levels

To investigate the effects of applied stresses on autogenous shrinkage and to determine the applicability of the basic creep model to low w/c concrete for various stress levels, autogenous shrinkage tests and basic creep tests were performed. Autogenous shrinkage strains were measured from 1 day after casting. Basic creep tests were performed with the following four stress levels applied at 1 day: $0.1f'_c$, $0.2f'_c$, $0.3f'_c$, and $0.4f'_c$.

Autogenous shrinkage strains were measured from embedded strain gages placed at the center of 100 mm × 100 mm × 400 mm prism specimens and ϕ150 mm × 300 mm cylindrical

Table 1
Concrete mixture proportions

w/c	s/a	Unit weight (kg/m^3)				Ad[a] (%)
		W	C	S	G[b]	
0.3	0.37	175	583	591	999	1.0
0.4	0.40	175	438	687	1031	0.6
0.5	0.42	175	350	752	1031	0.3
0.6	0.45	175	292	849	1030	0.1

[a] Superplasticizer (high-range water-reducing admixture), ratio of cement weight.
[b] Maximum aggregate size of 19 mm.

Table 2
Test specimens used to evaluate the effects of w/c and age, and stress level

Effect	Autogenous shrinkage test		Basic creep test ϕ150 mm × 300 mm cylinders	Compressive strength test ϕ150 mm × 300 mm cylinders
	100 mm × 100 mm × 400 mm prism	ϕ150 mm × 300 mm cylinders		
w/c and age	2	–	12	12
Stress level [a]	2	2	12	6

[a] Due to the limitation of our testing devices, the specimens for autogenous shrinkage and basic creep tests for various load levels were prepared on different days than were specimens of the preceding section with a w/c of 0.30.

specimens. Two types of specimen shapes were used to compare the difference of autogenous shrinkage strains with each specimen shape.

For the basic creep test in this section, we used the same procedure as in the preceding section. To measure the internal temperature changes in the specimens, thermocouples were embedded in all the autogenous shrinkage test specimens as well as in the basic creep test specimens. Applied loads for each stress level were measured from the load cell attached to the creep test device. Fig. 3 shows the experimental set-up for measuring autogenous shrinkage and basic creep. As in the two previous sections, we excluded the thermal strain from the corresponding measured strains to obtain the autogenous shrinkage strains and the basic creep strains.

3. Experiment results and analyses

3.1. Autogenous shrinkage tests and basic creep tests for various water/cement ratios and ages

Compressive strength and autogenous shrinkage results as a function of w/c and age are shown in Table 3 and Fig. 4, respectively. Autogenous shrinkage is an averaged value from the testing of two identical prism specimens in the series. Fig. 4 shows that most of autogenous shrinkage was produced within 5 days, and that autogenous shrinkage increases as the w/c decreases. More specifically, autogenous shrinkage is particularly at a high level when the w/c is 0.30. Autogenous shrinkage results produced from 1 day to 50 days and from 0 day to 50 days as the w/c increases are shown in Table 4. These results show that the influence of autogenous shrinkage is significant for the early ages of normal-strength concrete (NSC), for example within 5 days after placement, as well as for high-strength concrete (HSC).

The total strain of a concrete specimen measured from the basic creep test can be expressed as follows:

$$\varepsilon_{\text{total}}(t,\ t') = \varepsilon_{\text{elastic}}(t') + \varepsilon_{\text{creep}}(t,\ t') + \varepsilon_{\text{autogenous}}(t,\ t') \qquad (1)$$

where $\varepsilon_{\text{total}}(t, t')$ is the total strain, $\varepsilon_{\text{elastic}}(t')$ is the initial elastic strain, $\varepsilon_{\text{creep}}(t, t')$ is the creep strain, and $\varepsilon_{\text{autogenous}}(t, t')$ is the autogenous shrinkage strain at time t caused by an amount of constant stress applied at age t'.

As is well known, the current prediction model for basic creep is restricted to the service stress range (or up to about $0.4f'_c$) in which creep is assumed to be linearly dependent on the applied stress. The creep compliance function is the total strain per unit of the applied stress. The apparent compliance function is defined as follows:

$$J_{\text{apparent}}(t,\ t') = \frac{\varepsilon_{\text{total}}(t,\ t')}{\sigma(t')}. \qquad (2)$$

In Eq. (1), $\varepsilon_{\text{elastic}}(t')$ and $\varepsilon_{\text{creep}}(t, t')$ are dependent on the applied stress, and $\varepsilon_{\text{autogenous}}(t, t')$ is a material property that is independent of the applied stress. In Section 3.2, we discuss in detail the independence of autogenous shrinkage from the applied stress. It is noted that the apparent compliance function, including $\varepsilon_{\text{autogenous}}(t, t')$, cannot be a pure strain induced by unit stress. Accordingly, the real compliance function is defined by subtracting autogenous shrinkage from the total strain. It is expressed as follows:

$$J_{\text{real}}(t,\ t') = \frac{\varepsilon_{\text{total}}(t,\ t') - \varepsilon_{\text{autogenous}}(t,\ t')}{\sigma(t')}. \qquad (3)$$

Fig. 5 shows apparent and real creep compliance functions with w/c and age. The differences between the real and apparent compliance functions for four mixtures are distinct when the stress is applied at 1 day and 3 days, but the difference becomes less pronounced when the stress is applied after 7 days.

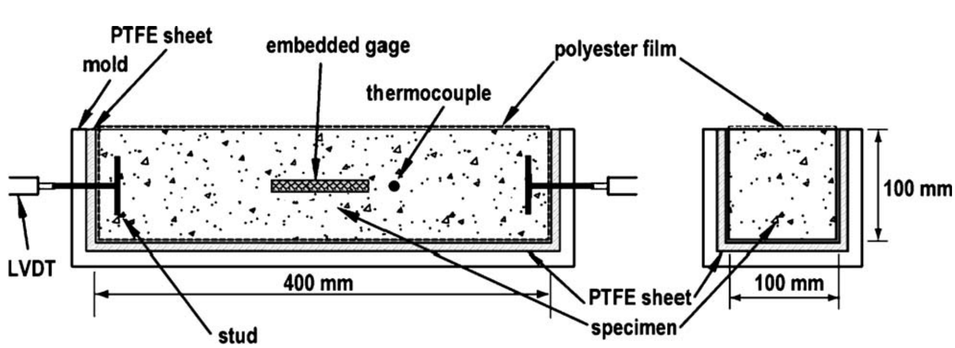

Fig. 2. Schematic diagram for measuring autogenous shrinkage of the concrete.

Fig. 3. The set-up for autogenous shrinkage tests and basic creep tests.

Westman [9], along with Østergaad et al. [10], extended the well-known basic creep model using the triple power law and solidification creep model to represent their basic creep test results at early ages in compression and tension. In their modification, autogenous shrinkage was not considered. Hence, for their modification on the basic creep model, they overestimated the compression and underestimated the tension in the basic creep strain. These differences may or may not cause important computational errors in thermal stress analyses. In stress analyses, the differences may prompt either an overestimation or underestimation of the real tensile stress produced by hydration heat. Besides the numerical errors in the computed stress values, the inclusion of autogenous shrinkage in a basic creep model can lead to a theoretical problem in concrete creep. We discuss this problem in the next section.

The results presented in this paper suggest that we should reconsider the effects of autogenous shrinkage, particularly at early ages of NSC and for low w/c concrete.

3.2. Autogenous shrinkage tests and basic creep tests for various stress levels

The average concrete compressive strength at 28 days was 57.9 MPa. For test specimens (Fig. 6) used to evaluate the influence of stress levels, the test results show that the effect of specimen shape on autogenous shrinkage is insignificant. Accordingly, in this study, we subtracted the autogenous shrinkage strains in the ϕ150 mm × 300 mm cylindrical specimens from the measured basic creep strains.

Fig. 7 shows the results of the autogenous shrinkage tests and basic creep tests for four stress levels. On the other hand, Figs. 7 (a) and (b) show the results before subtracting and after subtracting autogenous shrinkage, respectively. Although Figs. 7(a) and (b) have a similar shape, differences exist in the amount of creep strain and creep rate. Both the absolute creep strain and the creep rate play an important role in creep analyses, especially at early ages.

Fig. 8 shows the relationships between the total strains, including or excluding the autogenous shrinkage, and applied loads with age. In Fig. 8(a), the dashed line, which passes through an origin and the point corresponding to $0.1f_c'$ at $t-t'=$ 30 days, is above the points that correspond to $t-t'=30$ days for the other applied loads. In Fig. 8(b), however, the dashed line passes through the origin and the three points that correspond to $0.1f_c'$, $0.2f_c'$, and $0.3f_c'$ at $t-t'=30$ days. This result suggests that the creep strain shown in Fig. 8(a) is not directly proportional to the applied stress, but that the creep strain shown in Fig. 8(b) is proportional to the applied stress.

Table 3
Compressive strength results with w/c and age

w/c	Age (days)	f_c' (MPa)
0.3	1	23.57
	3	31.18
	7	39.27
	28	56.59
0.4	1	15.53
	3	24.49
	7	30.48
	28	42.36
0.5	1	9.49
	3	17.48
	7	25.36
	28	35.18
0.6	1	5.19
	3	11.48
	7	19.36
	28	26.45

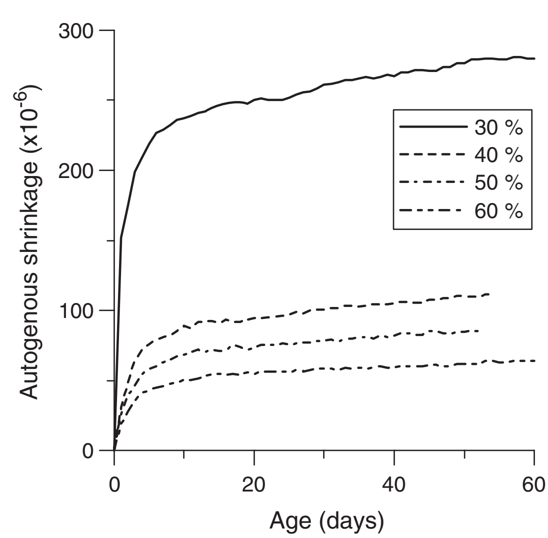

Fig. 4. Relationships between autogenous shrinkages and ages with w/c.

Table 4
Autogenous shrinkage results with age and w/c

Age (days)	w/c	Autogenous shrinkage ($\times 10^{-6}$)
From 0 to 50	0.3	270
	0.4	110
	0.5	80
	0.6	60
From 1 to 50	0.3	132
	0.4	85
	0.5	64
	0.6	45

From the results shown in Fig. 8, it can also be concluded that autogenous shrinkage is not nonlinearly dependent on the applied stress because the three points that correspond to the applied stresses $0.1f'_c$, $0.2f'_c$, and $0.3f'_c$ show a linear relationship. The term 'not nonlinear dependence' in this paper means that autogenous shrinkage is independent of the applied stress or, if present, autogenous shrinkage may be linearly dependent on the applied stress. More specifically, if autogenous shrinkage nonlinearly depends on the applied stress, a nonlinear relationship would occur in Fig. 8(a) or (b). The fact that autogenous shrinkage is not nonlinearly dependent on the applied stress is a very significant feature for predicting inelastic deformations such as creep or shrinkage. This will be explained in later this section.

For stresses within the service range, or up to approximately 40% of the strength, we assume that creep in concrete is approximately proportional to the stress. In this case, we can easily separate autogenous shrinkage in stress-free state from the total deformation measured from the basic creep test. If

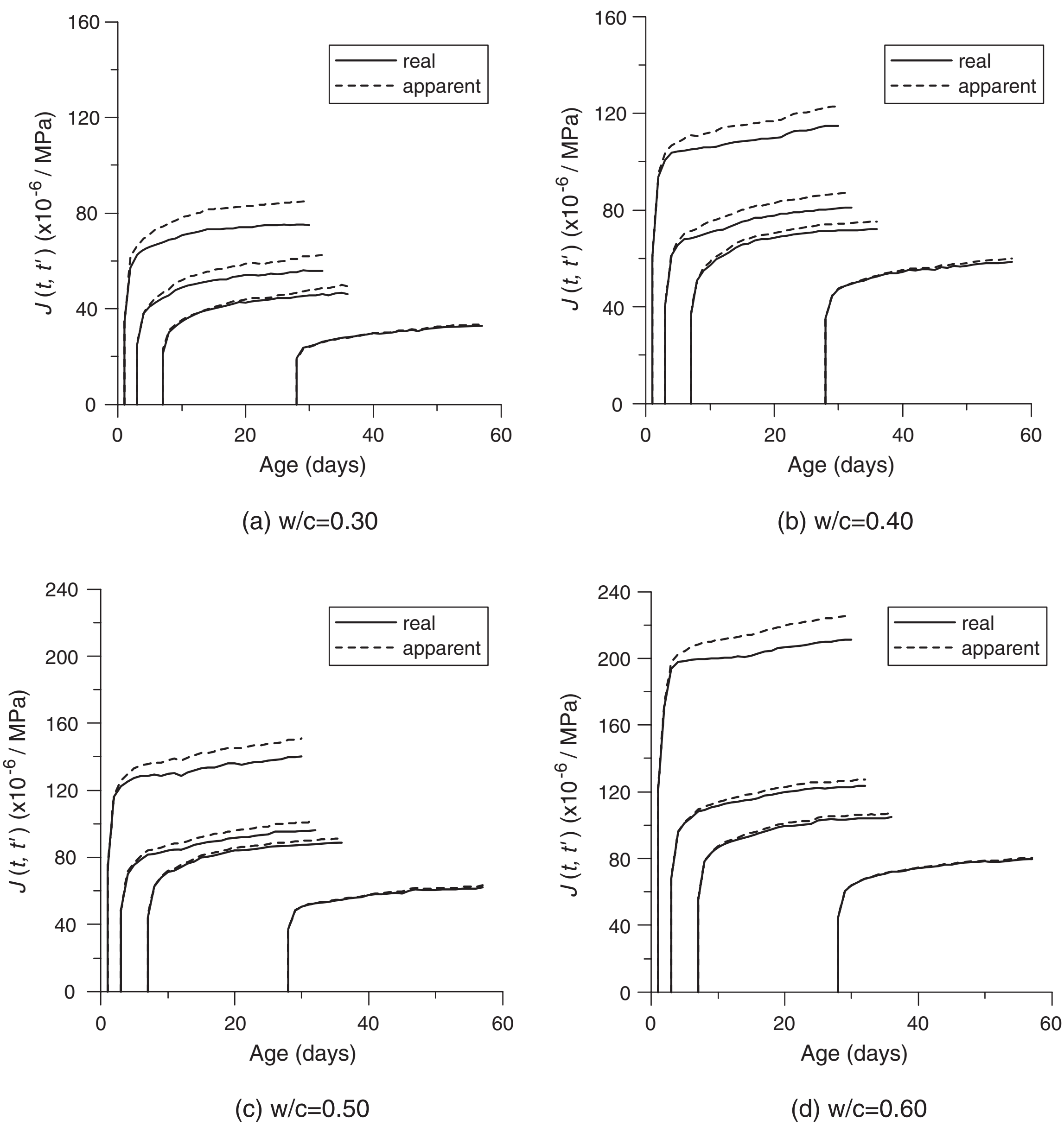

Fig. 5. Apparent and real creep compliance functions for various w/c ratios.

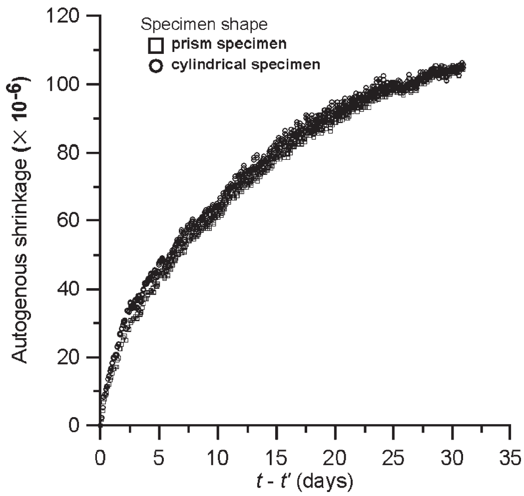

Fig. 6. Autogenous shrinkages with specimen shape.

autogenous shrinkage can not be separated from the measured creep strain, the well-known assumption may be invalid. In the case of $0.4f_c'$, however, a different trend occurred. This is because, for concrete at age one day, the application of a high stress such as $0.4f_c'$ may cause a nonlinear creep. Where the nonlinear creep means the creep strain, which does not proportional to the applied stress. Accordingly, the point corresponding to $0.4f_c'$ does not lie on the line dissimilarly to three points in Fig. 8(b). Discussion regarding the occurrence of this nonlinear behavior is, however, outside the scope of this paper.

3.3. Deformation components of drying and sealed specimens

Fig. 9 shows the deformation components of drying and sealed specimens under applied stresses. Generally, the total deformations of a drying specimen are composed of basic creep, drying shrinkage, and drying creep. The very significant proposal to distinguish clearly between phenomena induced by distinct causes, namely, basic creep and drying creep, was first alluded to by Neville [17] in 1955, introduced by Hansen [18] in the interpretation of creep, and fully validated by Ali and Kesler [19] by 1964. In this context, drying creep designates the increase in creep strain resulting from the drying process. Drying creep is ascribed to an accelerated movement of water molecules in the pore system of the hydrated cement paste caused by the external load. Thus, this term is used in current model codes such as ACI [20], CEB-FIP [21], and model B3 [22]. We therefore postulate that, under the same consideration as the drying specimen, the total deformations of a sealed specimen are composed of real basic creep, autogenous shrinkage, and, if present, several other stress-dependent terms.

Autogenous shrinkage strains measured in conventional tests are strains produced in a stress-free state. Accordingly, we cannot recognize the existence of a stress-dependent term from such a stress-free test. However, as previously mentioned, Fig. 8 suggests that autogenous shrinkage is not nonlinearly dependent on the applied stress. Actually, from the test results performed in this study, it was not determined whether autogenous shrinkage linearly depends on the applied stress or if it does not. However, the dependence does not make a problem in obtaining the creep model and using it to predict concrete creep behavior. If autogenous shrinkage is independent of the applied stress, then there is no problem, we can subtract directly autogenous shrinkage from the basic creep test results. If autogenous shrinkage is linearly dependent on the applied stress, we can add this proportional shrinkage shown in Fig. 9 to the real basic creep. In this case, the proportional stress-dependent term is considered as stress-induced autogenous shrinkage like creep. Since autogenous shrinkage always happens in every concrete specimen, unlike drying creep, current model codes such as ACI [20], CEB-FIP [21], and model B3 [22] have accounted for stress-induced autogenous shrinkage. Even if this is true, it seems reasonable to predict concrete creep behavior using those model codes as

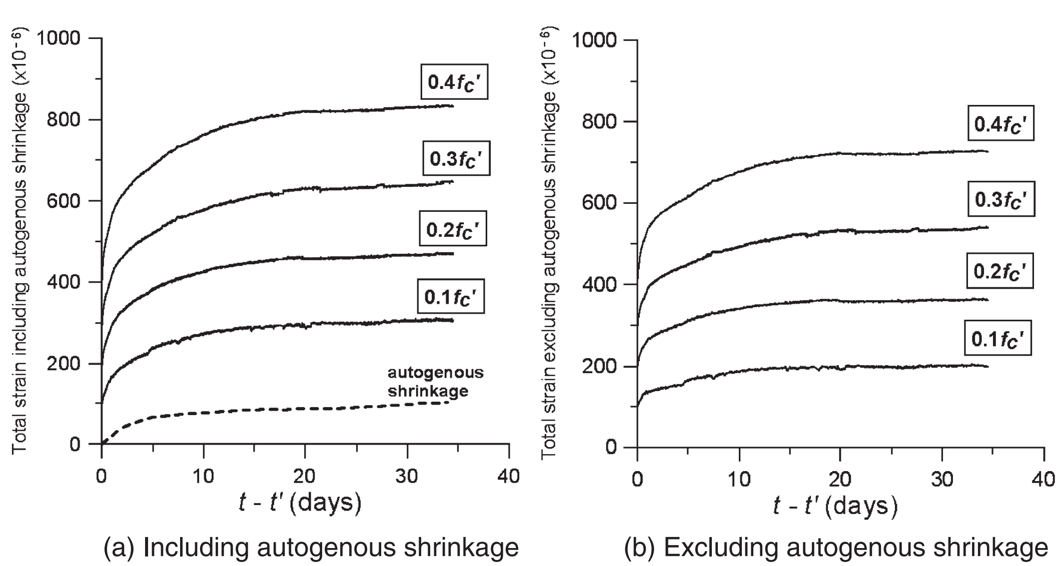

Fig. 7. Relationships between total strains and ages with load level.

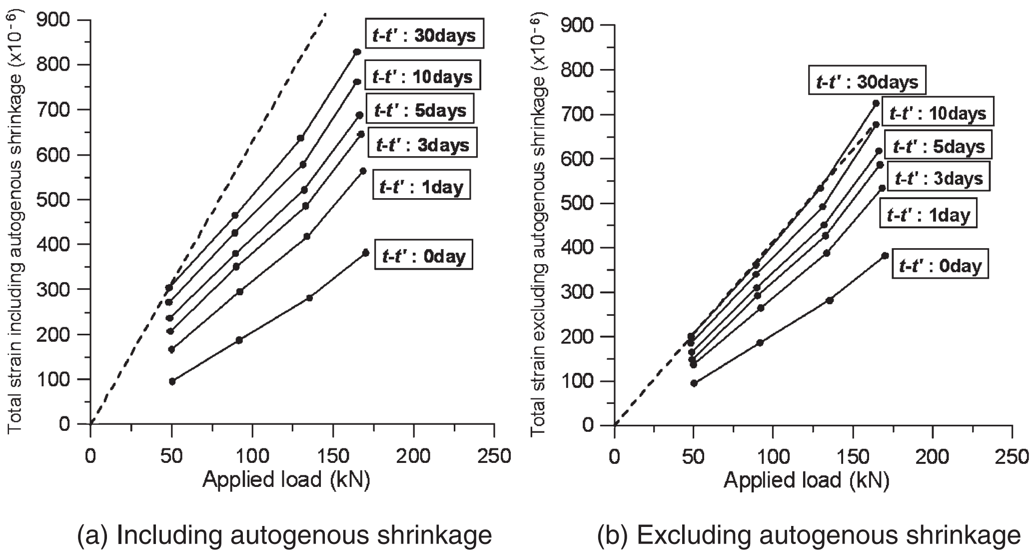

Fig. 8. Relationships between total strains and applied loads with age for basic creep test.

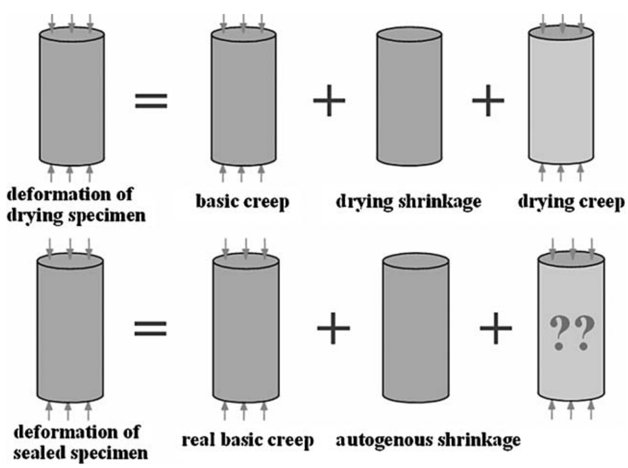

Fig. 9. Comparison of the deformation between drying and sealed specimens.

long as the autogenous shrinkage portion irrelevant to the applied stress is separated from total deformations, as stress-induced autogenous shrinkage is proportional to the applied stress and we can obtain the creep compliance function independent of the applied stress. Hence, there is no need to develop the additional stress-induced autogenous shrinkage model such as the drying creep model for predicting overall creep deformations. Accordingly, in this case, we have only to subtract stress-free autogenous shrinkage from the basic creep test results as in the previous case.

We therefore conclude that the real creep compliance function shown in Eq. (3) can be obtained from the total strains

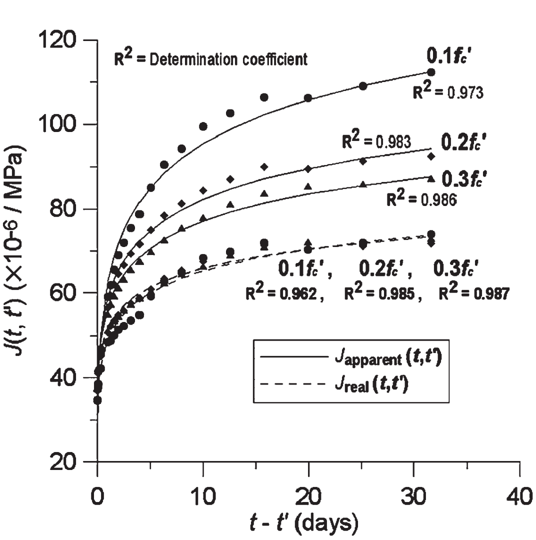

Fig. 10. Apparent and real creep compliance functions with age.

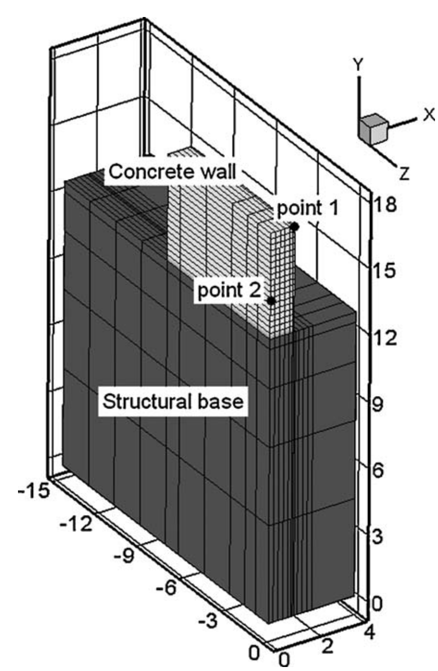

Fig. 11. Configuration and mesh modeling.

Table 5
Input data for thermal stress analyses

Parameter	
Cement content (kg/m^3)	438
Specific heat (J/kgK)	962.96
Thermal conductivity (W/mK)	2.326
Density (kg/m^3)	2320
Convective heat transfer coefficient (W/m^{2}K)	17.445

measured in conventional basic creep tests by simply subtracting the autogenous shrinkage strains in a stress-free state.

3.4. Experimental data and results of the apparent and real creep compliance functions

Fig. 10 shows the experimental data and results of the apparent and real creep compliance functions derived from Eqs. (2) and (3) for all specimens. In Fig. 10, the test results of the apparent and real creep compliance functions were calibrated by Eq. (4) [23]. Eq. (4) is expressed as follows:

$$J(t,\ t') = p_1 + p_2 F(t,\ t'), \tag{4}$$

where $F(t,\ t')=C_0(t,\ t')$ is the compliance function for basic creep as proposed in model B3 [22]; $J(t,\ t')$ represents the test results, and p_1 and p_2 represent the update parameters.

Fig. 10 shows that for the apparent creep compliance function there were considerable differences with stress level. However, for the real creep compliance function, this difference is very small. Accordingly, the real creep compliance function, which is independent of the applied stress, can be regarded as a creep compliance function that is applicable to creep analyses.

Creep models recommended by existing model codes such as ACI [20], CEB-FIP [21], and model B3 [22] suggest only one creep compliance function that is independent of the applied stress: namely, the $J(t,\ t')$ value. The uniqueness of $J(t,\ t')$ enables us to easily apply a step-by-step method to creep analyses. In the step-by-step method, we can obtain the total strain $\varepsilon(t_n)$ at age t_n from the following equation using the unique $J(t_n,\ t_i)$, regardless of the stress increment $\Delta\sigma(t_i)$ applied at time t_i:

$$\varepsilon(t_n) = \sigma(t_0)J(t_n,\ t_0) + \sum_{i=1}^{n-1} \Delta\sigma(t_i)J(t_n,\ t_i). \tag{5}$$

However, if $J(t_n,\ t_i)$ is dependent on $\Delta\sigma(t_i)$, it will cause serious problems. First, it is computationally more difficult to store all the $J(t_n,\ t_i)$ values that depend on $\Delta\sigma(t_i)$ as the time step increases. Second, as $J(t_n,\ t_i)$ becomes a function of $\Delta\sigma(t_i)$, the problem becomes more complex and nonlinear. Accordingly, to avoid these two possibilities in practice, we recommend obtaining the creep compliance function $J(t,\ t')$ independent of the applied stress.

4. Analysis example for the evaluation of creep model

The type of structure selected as an example to perform thermal stress analyses in this section would be similar to the massive concrete wall of a nuclear power plant (NPP) intake structure. The specimen shown in Fig. 11 is a concrete wall sized 14.6 m length × 4.8 m height × 2.23 m thickness, correspondingly. Only a quarter of the specimen needs to be considered due to symmetry. Input data for thermal stress analyses of such a concrete wall are shown in Table 5.

The temperature distribution for w/c = 0.3 and w/c = 0.4 at 1.75 days are shown in Figs. 12(a) and (b), respectively. 1.75 days was selected as, at that time, it shows the maximum temperature. For the adiabatic temperature rise

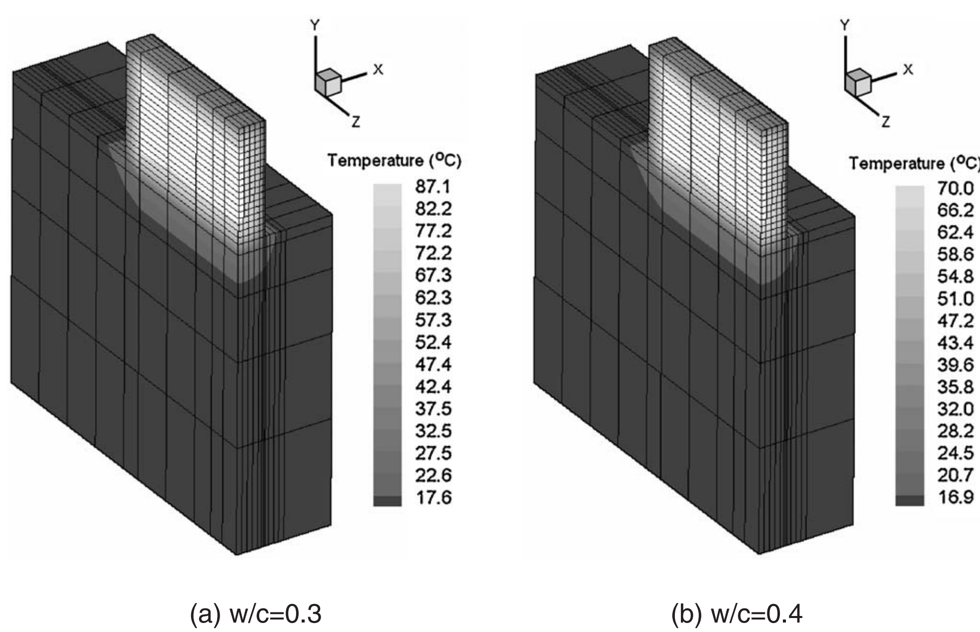

Fig. 12. Temperature distributions at 1.75 days.

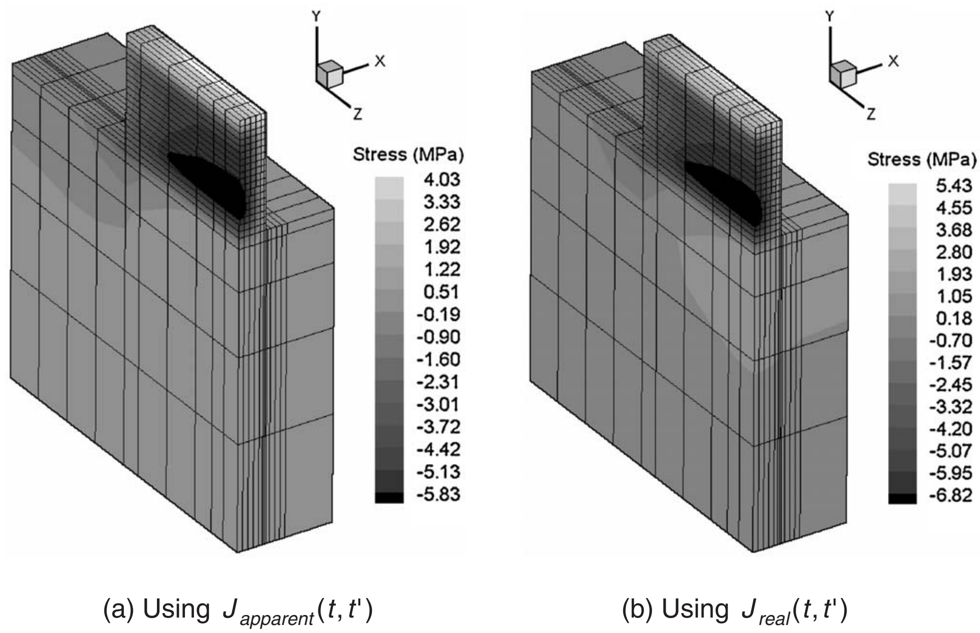

Fig. 13. Stress distributions in Z-direction at 1.75 days (w/c = 0.3).

curve with w/c, the equation (i.e., Eq. (6)) by Ohzawa [23] was used.

$$T = K[1 - e^{-\alpha t}] \tag{6}$$

where T is the adiabatic temperature rise at time t (°C), K is the maximum adiabatic temperature rise (56.6 °C), α is the temperature increasing velocity (0.705), and t is the time (day). In addition, water cementitious materials ratio (w/cm) and ambient temperature are 0.44 and 15 °C, respectively. In this example, by using apparent $J(t_n, t_i)$ and real $J(t_n, t_i)$ obtained from Eqs. (2) and (3), respectively, the thermal analyses were performed. Namely, apparent $J(t_n, t_i)$ and real $J(t_n, t_i)$ mean the compliance values, respectively, including and excluding stress-free autogenous shrinkage.

Figs. 13 and 14 show the thermal stress distributions for w/c = 0.3 and w/c = 0.4 at 1.75 days, respectively. Model B3 was used to obtain the compliance function [22,24]. For w/c = 0.3%, the difference between tensile stresses of both cases (i.e., apparent $J(t_n, t_i)$ and real $J(t_n, t_i)$) at the external surface (point 1) is distinct. In addition, for w/c = 0.4%, the difference is not negligible.

Autogenous shrinkage always has a negative value. Accordingly, when apparent $J(t_n, t_i)$ obtained from compressive creep tests is used, the tensile stress at the external surface has a

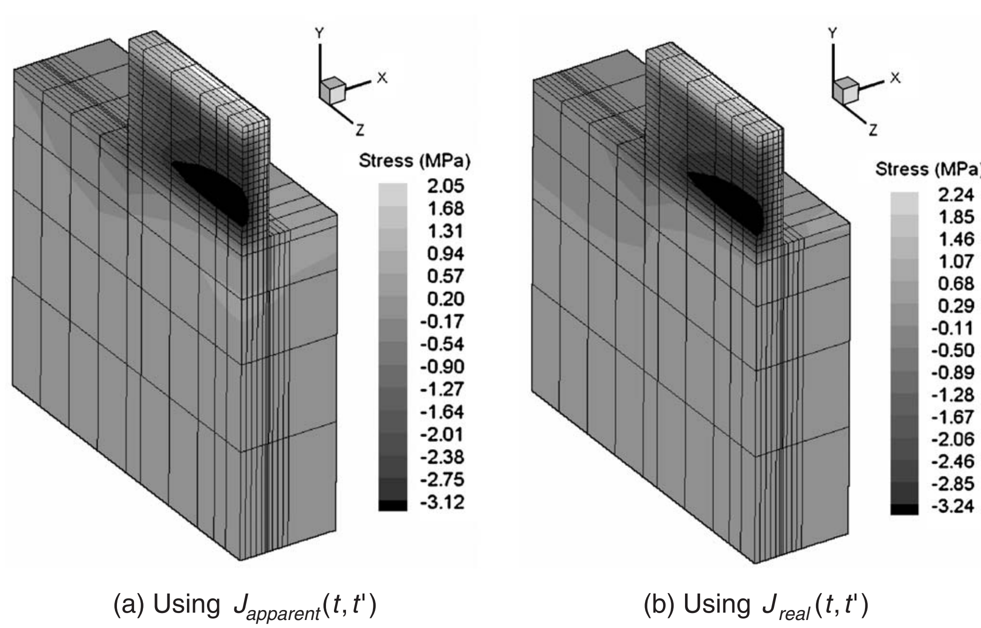

Fig. 14. Stress distributions in Z-direction at 1.75 days (w/c = 0.4).

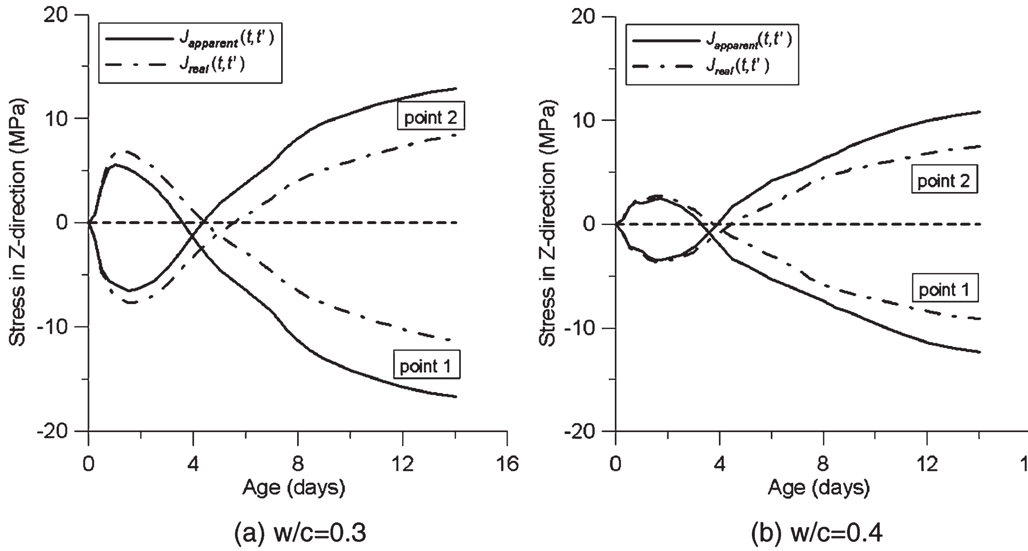

Fig. 15. Thermal stress histories in *Z*-direction at two points of the concrete wall.

smaller value than that for real $J(t_n, t_i)$ since apparent $J(t_n, t_i)$ is higher than real $J(t_n, t_i)$. Meanwhile, under the tensile creep tests, contrary results may occur; for instance, the stress for apparent $J(t_n, t_i)$ has a larger value compared to that for real $J(t_n, t_i)$. To obtain more reasonable analysis results, real $J(t_n, t_i)$ subtracted autogenous shrinkage from apparent $J(t_n, t_i)$ should be used. When autogenous shrinkage is included in $J(t_n, t_i)$, it is possible to obtain incorrect results.

Figs. 15(a) and (b) show, respectively, the stresses in *Z*-direction for w/c = 0.3, and w/c = 0.4 at points 1 and 2 of Fig. 11. Expectedly, the actual tensile stress at the surface (point 1) at early ages when real $J(t_n, t_i)$ was used is greater than that of the apparent $J(t_n, t_i)$ case. Accordingly, it can be concluded that, if autogenous shrinkage is not subtracted in the calculation of the creep compliance function, the tensile stress can be underestimated and, as a result, a very serious error can occur. The differences in thermal stresses between the two cases become greater as the time increases. At 14 days, the differences in tensile stresses at point 2 are 4.4 MPa and 3.4 MPa, respectively, for w/c = 0.3 and w/c = 0.4. These facts make it difficult to predict the passing through thermal cracks occurred in massive concrete structures.

Finally, it is noted that the method excluding stress-free autogenous shrinkage from measured basic creeps can reduce the incidence of errors in the thermal stress analyses and produce more accurate results. This approach is a necessary method and should be considered important in the basic creep models used currently.

5. Conclusions

In this study, the effect of autogenous shrinkage on the basic creep model equation of concrete was examined. The conclusions obtained from this study can be summarized as follows:

1. Autogenous shrinkage is definitely present and not negligible for low w/c concrete and at early ages of NSC.
2. For early loading stages, distinct differences occur in the apparent and real creep compliance functions. The importance of these differences increases as the w/c of the concrete decreases.
3. Autogenous shrinkage is not nonlinearly dependent on the applied stress, and stress-free autogenous shrinkage should be separated from basic creep test results to obtain a basic creep model for prediction of concrete creep deformations in the numerical stress analyses, for example, in thermal stress analyses and crack control problems.

Acknowledgements

This research was supported by the National Research Laboratory (NRL) program, under the Korean Ministry of Science and Technology, for the development of the cracking control technique of concrete structures.

References

[1] C.G. Lyman, Growth and Movement in Portland Cement Concrete, Oxford University Press, London, UK, 1934, pp. 1–139.

[2] E. Tazawa, S. Miyazawa, T. Sato, K. Konishi, Autogeneous shrinkage of concrete, Proc. Jpn. Concr. Inst. 14 (1) (1992) 561–566.

[3] E. Tazawa, S. Miyazawa, Influence of cement and admixtures on autogenous shrinkage of cement paste, Cem. Concr. Res. 25 (2) (1995) 281–287.

[4] O.M. Jensen, P.F. Kansen, Autogenous deformation and change of the relative humidity in silica fume-modified cement paste, ACI Mater. J. 93 (6) (1996) 539–543.

[5] A. Radocea, Autogenous volume change of concrete at very early age, Mag. Concr. Res. 50 (2) (1998) 107–113.

[6] S.N. Lim, T.H. Wee, Autogeneous shrinkage of ground-granulated blast-furnace slag concrete, ACI Mater. J. 97 (5) (2000) 587–593.

[7] E. Tazawa, S. Miyazawa, Autogeneous shrinkage caused by self desiccation in cementitious material, 9th International Congress on the Chemistry of Cement, 1992, pp. 712–718.

[8] Japan Concrete Institute, Report of the technical committee on super-workable concrete, Part 2 (in Japanese).

[9] G. Westman, Basic creep and relaxation of young concrete, in: R. Springenschmidt (Ed.), Thermal Cracking in Concrete at Early Ages,

Proceedings of the International RILEM Symposium, E&FN Spon, London, 1995, pp. 87–94.
[10] L. Østergaad, D.A. Lange, S.A. Altoubat, H. Stang, Tensile basic creep of early-age concrete under constant load, Cem. Concr. Res. 31 (12) (2001) 1895–1899.
[11] S.A. Altoubat, D.A. Lange, Tensile basic creep: measurements and behavior at early age, ACI Mater. J. 98 (5) (2001) 386–393.
[12] S.A. Altoubat, D.A. Lange, The Pickett effect at early age and experimental separating its mechanisms in tension, Mat. Struct. 35 (248) (2002) 211–218.
[13] A.D. Ross, Creep of concrete under variable stress, J. Am. Concr. Inst. 54 (1958) 739–758.
[14] U.S. Bureau of Reclamation, Supplement Report – 5-year creep and strain recovery of concrete for Hungry Horse Dam, Concrete Laboratory Report No. C-179A (Denver, Colorado, 6 Jan. 1959).
[15] American Society for Testing and Materials. Standard specification for chemical admixtures for concrete, ASTM C 494-99, Philadelphia.
[16] American Society for Testing and Materials. Standard test method for compressive strength of cylindrical concrete specimens, ASTM C 39-01, Philadelphia.
[17] A.M. Neville, Theories of creep in concrete, J. Am. Concr. Inst. 52 (1955) 47–60.
[18] T.C. Hansen, Creep of concrete, a discussion of some fundamental problems, Bulletin No. 33 of the Swedish Cement and Concrete Institute at the Royal Institute of Technology, Stockholm, 1958.
[19] J. Ali, C.E. Kesler, Mechanisms of creep in concrete, Symposium of Creep of Concrete, ACI Special Paper, No. 9, Detroit, 1964.
[20] ACI Committee 209, Prediction of creep, shrinkage, and temperature effects in concrete structures, ACI Manual of concrete practice, Part 1, ACI, 1999.
[21] CEB-FIP, Model Code for Concrete Structures (MC-90), CEB, Thomas Telford, London, 1993, 112 pp.
[22] RILEM TC 107, Creep and shrinkage prediction model for analysis and design of concrete structures – model B3 (chaired by Bazant Z. P.), Mat. Struct. 28 (180) (1995) 365.
[23] S. Ohzawa, Study on the reduction of early age cracking of massive concrete (I), Report No. 57 (1962) (in Japanese).
[24] Z.P. Bazant, S. Baweja, Justification and refinements of model B3 for concrete creep and shrinkage: 2. Updating and theoretical basis, Mat. Struct. 28 (182) (1995) 488–495.